DE GRUYTER
OPEN
10.1515/tvsb-2016-0009

Transactions of the VŠB – Technical University of Ostrava
Civil Engineering Series, Vol. 16, No. 2, 2016
paper #9

Radek DUBINA [1], Jan ELIÁŠ [2]

EFFECT OF ROLLING RESISTANCE IN DEM MODELS WITH SPHERICAL BODIES

Abstract

The rolling resistance is an artificial moment arising on the contact of two discrete elements which mimics resistance of two grains of complex shape in contact rolling relatively to each other. The paper investigates the influence of rolling resistance on behaviour of an assembly of spherical discrete elements. Besides the resistance to rolling, the contacts between spherical particles obey the Hertzian law in normal straining and Coulomb model of friction in shear.

Keywords

Discrete element method (DEM), contact law, rolling resistance, experimental results.

1 INTRODUCTION

Many different methods have been developed for solution of various engineering problems, among which the Discrete Element Method (DEM) is suitable for modelling of granular media. In the DEM, every grain of the assembly is represented by an ideally rigid and independent body which can interacts with the other bodies through forces and moments at their contacts. It has been reported that shape of the grains is of extreme importance [8]. Therefore, complex and realistic shapes are often used in simulation, for example discrete ellipsoids [4], tetrahedrons [18], polyhedrons [1, 5] or clumps of smaller spherical particles [6, 7, 17].

However, the complex shapes of the bodies require much longer computational time to detect and characterize the contact between them. In order to speed up significantly the simulation that involves many bodies, spherical shapes are typically used instead. The shape simplification can be phenomenologically compensated by adding rolling resistance on the contact of spherical particles [2, 10, 11].

This contribution focuses on the parameters of the rolling resistance. It presents simulation of the shear test, oedometric test and composite element test. All the calculations are performed in the open-source software Yade [16] using spherical elements with the Hertz-Mindlin contact type [14].

2 CONTACT LAWS

In this section, the constitutive formulas of the spherical contact are introduced. The section is written according to the Yade manual and its source code. It is convenient to start with definition of few auxiliary variables. Let us assume there are two spheres, A and B, in a contact. Each of the sphere has its own radius (R_a, R_b), Young's modulus (E_a, E_b) and Poisson's ratio (ν_a, ν_b). The shear modulus for each body is obtained from

$$G_i = \frac{E_i(1+\nu_i)}{2} \tag{1}$$

[1] Ing. Radek Dubina, Institute of Structural Mechanics, Faculty of Civil Engineering, University of Technology Brno, Veveří 331/95, 602 00 Brno, Czech Republic, phone: (+420) 541 147 378, e-mail: dubina.r@fce.vutbr.cz.

[2] Ing. Jan Eliáš, Ph.D., Institute of Structural Mechanics, Faculty of Civil Engineering, University of Technology Brno, Veveří 331/95, 602 00 Brno, Czech Republic, phone: (+420) 541 147 132, e-mail: elias.j@fce.vutbr.cz.

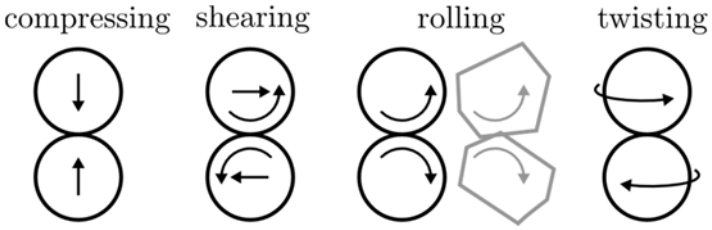

Fig. 1: Schematic plot of relative movements of two spheres in contact

The effective Young's modulus, E_{eff}, the effective shear modulus, G_{eff}, and effective Poisson's ratio, ν_{eff}, of the contact are given by

$$E_{\text{eff}} = \frac{E_a E_b}{(1-\nu_a^2)E_b + (1-\nu_b^2)E_a}, \tag{2}$$

$$G_{\text{eff}} = \frac{G_a + G_b}{2}, \tag{3}$$

$$\nu_{eff} = \frac{\nu_a + \nu_b}{2}. \tag{4}$$

Two types of radii are used, the mean radius, R_{mean}, and the equivalent radius, R_{eq},

$$R_{mean} = \frac{R_a + R_b}{2}, \tag{5}$$

$$R_{eq} = \frac{R_a R_b}{R_a + R_b}. \tag{6}$$

In every time step, relative movements of the two spheres are decomposed into normal deformation, u_{N}, shear deformation u_{T}, rolling angle ω_{R} and twist angle ω_{T}, see Fig. 1. Based on these quantities, the forces and moments on the contact arise. The twisting is omitted in the current formulation.

2.1 Normal direction

There is no cohesion included and therefore no tensile force arising between the spheres for $u_{\text{N}} < 0$. In compression ($u_{\text{N}} > 0$), the Hertzian contact is applied

$$\boldsymbol{F}_N = \boldsymbol{n}\, k_N \sqrt{{u_N}^3}. \tag{7}$$

Where $\boldsymbol{n}$ is a normal between two bodies and k_{N} [$\text{N/m}^{3/2}$] is the normal stiffness

$$k_N = \frac{4}{3} E_{eff} \sqrt{R_{eq}}. \tag{8}$$

2.2 Tangential direction

The shear force F_{T} is calculated by standard incremental algorithm [14, 15]. It involves the correction of the shear force from the previous time step for changes in the normal direction and for particle motion. Incremental shear displacement caused by the mutual movements and rotations of bodies, Δu_{T}, is calculated and the shear force is adjusted by the following increment

$$\Delta \boldsymbol{F}_T = k_T \Delta \boldsymbol{u}_T, \tag{9}$$

where k_{T} [N/m] is the shear stiffness of the material [15]

$$k_T = \frac{4 G_{eff} \sqrt{R_{eq}}}{2 - \nu_{eff}} \sqrt{u_N}. \tag{10}$$

Coulomb friction limit is enforced, the maximal magnitude of the shear force is restricted by the following condition

$$\|\boldsymbol{F}_T\| \leq \|\boldsymbol{F}_N\| \tan\varphi \tag{11}$$

with φ being the angle of internal friction.

2.3 Rolling

Rolling resistance [2, 10, 16] is an artificial moment arising on the contact of two discrete elements that mimics resistance of two grains of complex shape in contact rolling relatively to each other. It is necessary to use rolling resistance when spherical elements are employed to reproduce behaviour of non-spherical particles such as grains in railway ballast. The model of rolling resistance assumes linear dependence of the rolling moment increment, $\Delta\boldsymbol{\omega}_{\mathrm{R}}$, on the rolling angle increment, $\Delta\boldsymbol{M}_{\mathrm{R}}$, via the stiffness in rolling, k_{R} [Nm]

$$\Delta\boldsymbol{M}_R = k_R \Delta\boldsymbol{\omega}_R. \tag{12}$$

The stiffness in rolling is calculated based on parameter α_{R} [-]

$$k_R = \alpha_R E_{eff} R_{mean}^3 \nu_{eff}. \tag{13}$$

Similarly to the shear, the upper limit is imposed on the rolling moment magnitude.

$$\|\boldsymbol{M}_R\| \leq \mu_R \|\boldsymbol{F}_N\| R_{mean} \tag{14}$$

Parameter μ_R [-] controls the maximum rolling moment similarly to the tangent of internal friction angle in shear.

3 SIMULATIONS OF LABORATORY EXPERIMENTS

The influence of coefficients α_{R} and μ_{R} is studied in the DEM simulations of laboratory experiments. The aim is to identify suitable values of these coefficients. Remaining material properties for all the simulations are listed in Table 1.

Tab. 1: Material properties used in simulations of laboratory experiments

Ballast	Young's modulus	E	Pa	7.0×10^{10}
	Poisson ratio	ν	-	0.3
	Density	ρ	kg/m^3	2600.0
	Friction angle	φ	rad	0.5
Steel	Young's modulus	E	Pa	70.0×10^{10}
	Poisson ration	ν	-	0.25
	Density	ρ	kg/m^3	7850.0
	Friction angle	φ	rad	0.0 (0.5)

3.1 Oedometric test

The first simulation is a large-scale oedometric test on railway ballast performed at the University of Nottingham by Lim [12]. The dimensions of the oedometric test are d = 300 mm in diameter and h = 150 mm in depth. The boundary conditions of rigid non-deformable cylinder are shown in the Fig. 2 (markers ⊥, ○ or dots in the floor projection).

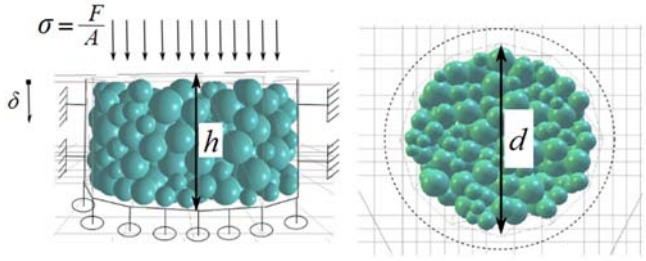

Fig. 2: Scheme of the oedometric test arrangement

The simulation proceeds as follows. The oedometer is filled by spherical bodies representing individual grains of the gravel. The diameters of spheres are sampled randomly from uniform distribution in range 20.5 and 44.5 mm. Such sampling provides reasonable agreement with a sieve curve of the real material while the sampling technique is kept simple. The sample is vibrated by alternating horizontal acceleration to provide sufficient amount of contacts. The sample is loaded by compressive force up to 1500 kN and then unload, the loading is defined by cosine function

$$F(t) = \frac{1500}{2}[1 - \cos(2\pi f t)], \tag{15}$$

where f is loading frequency and t is time. The loading frequency was 1 Hertz. The ballast material properties were set according to the literature and they are listed in Tab. 1. The oedometer was made from steel with zero friction angle [13].

Fig. 3 shows average value and standard deviation of displacement of the loading plate at the maximal compressive force. The statistics are computed for several considered variants of rolling parameters, each time out of 10 simulations differing in initial body locations and their diameters. The results show that parameters of the rolling resistance do not play a significant role in oedometric test. The sample is confined and the grains do not experience large mutual movements.

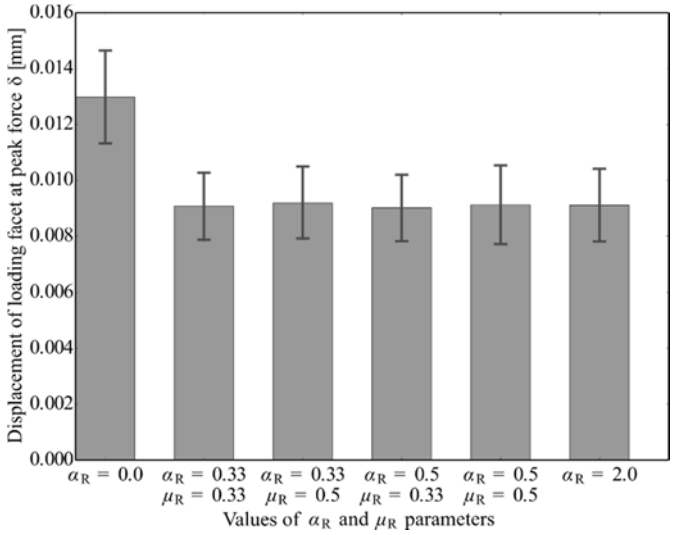

Fig. 3: Loading plate displacement at the peak force on different variants of rolling parameters; Average values and standard deviations are computed from 10 realizations

3.2 Composite element test (CET)

The second simulated experiment is called Composite element test (CET). This experiment was performed at the University of Nottingham [3]. At first the wooden box of size 1.4 × 0.7 m and depth 0.5 m was crafted. The wooden desks were covered by steel plates to decrease the friction between walls and ballast (friction angle 0.0 rad). Then the box was filled by the ballast in two differing arrangements/phases, but only the phase 1 is studied here, Fig. 4. The ballast was loaded by steel sleeper, which had dimensions 0.25 × 0.15 m, in number compressive cycles. The loading force in one cycle went from 1.0 kN up to 20.0 kN and then back.

The same material properties as in the oedometric test are used in the model (Tab. 1). The compaction of the sample was done via simulating one additional initial cycle that compacted the specimen, but this cycle is not included in the graphs described later. The statistics are computed for several considered variants of rolling parameters, each time out of 15 simulations differing in initial body locations and their diameters. The average vertical displacement of the loading sleeper after each cycle is measured and compared with the experimental results in Fig. 5.

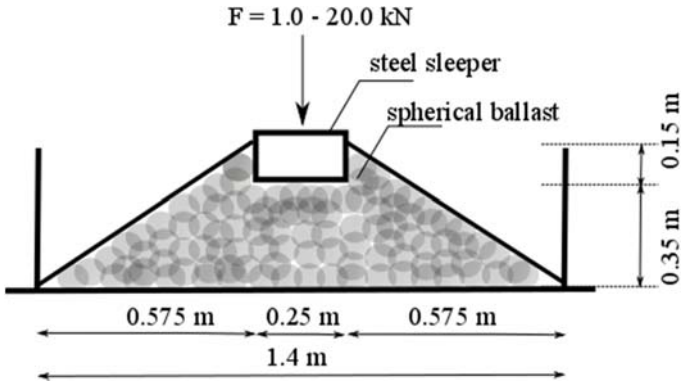

Fig. 4: Scheme of the Composite element test arrangement; The wooden box has dimensions 1.4 × 0.7 × 0.5 m; The ballast is cyclically loaded by steel sleeper within an interval from 1.0 to 20.0 kN

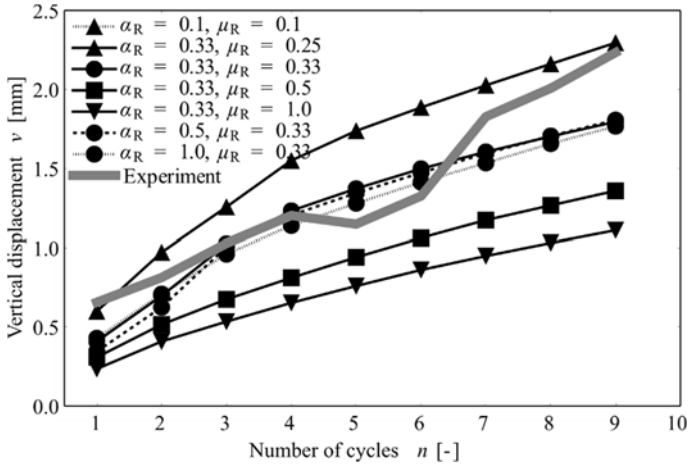

Fig. 5: Influence of rolling coefficients on vertical displacement of loading sleeper induced by cyclic loading

Fig. 5 shows results of several variants of rolling resistance. Each curve is an average of 15 realizations differing in initial locations of grains. The best agreement is achieved with $\mu_R = 0.33$ and the results seems to be independent on α_R. An example of force chain in the granular system is presented on the Fig. 6a, the loading is transferred mainly through few columns. The strength of the columns if governed by μ_R and for low values of this parameters, the deformations becomes excessively large. The sleeper penetrates into the gravel domain as shown in Fig. 6b.

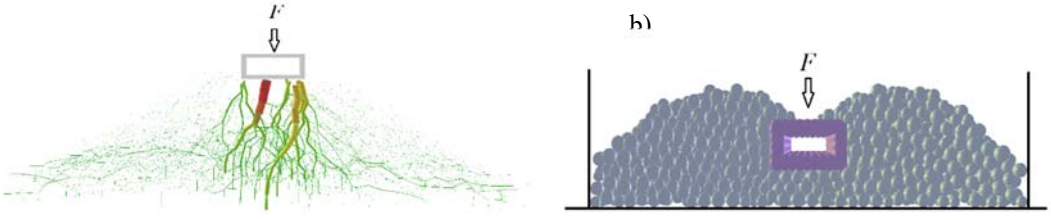

Fig. 6: a) force chains transferring load through the discrete system; b) penetration of the sleeper into the gravel domain for low value of μ_R coefficient

3.3 Shear test

Two different experimental shear tests are simulated using DEM. First was published in [9] and the dimensions of a large scale shear box (Fig. 7) were a = 300 mm, b = 300 mm, and c = d = 100 mm. A loading plate that allowed the particles to be displaced vertically during shearing was placed on the top and created upper boundary with additional surcharge. The box was filled by spherical discrete elements with mean diameter 35.0 mm. During the loading, the bottom part of the box is horizontally displaced while the upper part remains at the original position. The four levels of the vertical pressure were tested and modelled: 15, 27, 51 and 75 kPa.

The second shear test was published in [17]. The shear box dimensions are a = 360 mm, b = 300 mm, c = 160 mm and d = 80 mm, see Fig. 7. Higher levels of normal pressure are used, they are 100, 200 and 300 kPa, respectively.

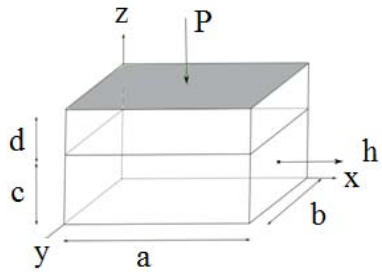

Fig. 7: Scheme of the shear test arrangement; The loading is realized by displacement of the lower part of box in horizontal direction, h, and surcharge at the top, P

10 realizations of every shear experiment are simulated differing in initial body locations and their diameters. The average shear stress S and vertical displacement v is measured. The Wang's shear test results are presented in Fig. 8. Four different values of rolling parameters are investigated. Studied parameters are displayed in legend of the graphs. The best agreement with experiment is achieved when $\mu_R = 0.1$. We can observe again that parameter α_R does not play a significant role. The simulations of Indaratna's shear test are presented in Fig. 9. Best agreement is again provided for $\mu_R = 0.1$. The values of μ_R lower than 0.1 have not been studied because, even if better match with shear tests is found, the CET test needs values of μ_R about 0.33. From both simulated shear experiments it is clearly seen that by increasing vertical pressure the lower value of μ_R is needed to obtaining better agreement between a simulation and the experiment.

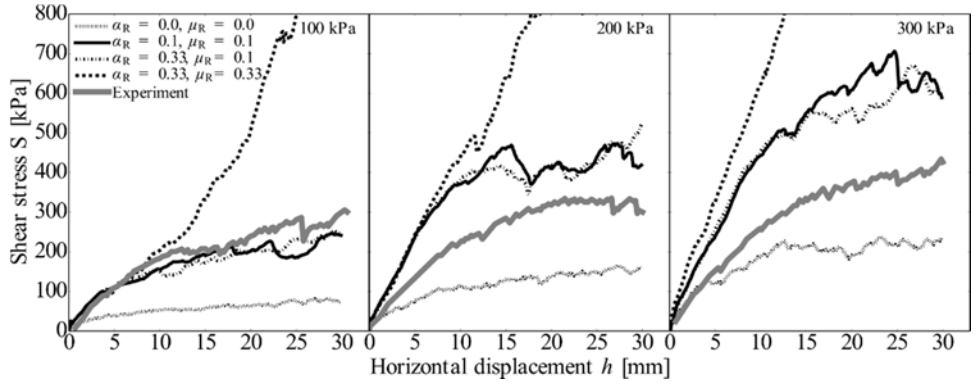

Fig. 8: The average responses from 10 realizations of Wang's shear test; The dependence of shear stress on horizontal displacement of lower box is shown for three vertical pressure values

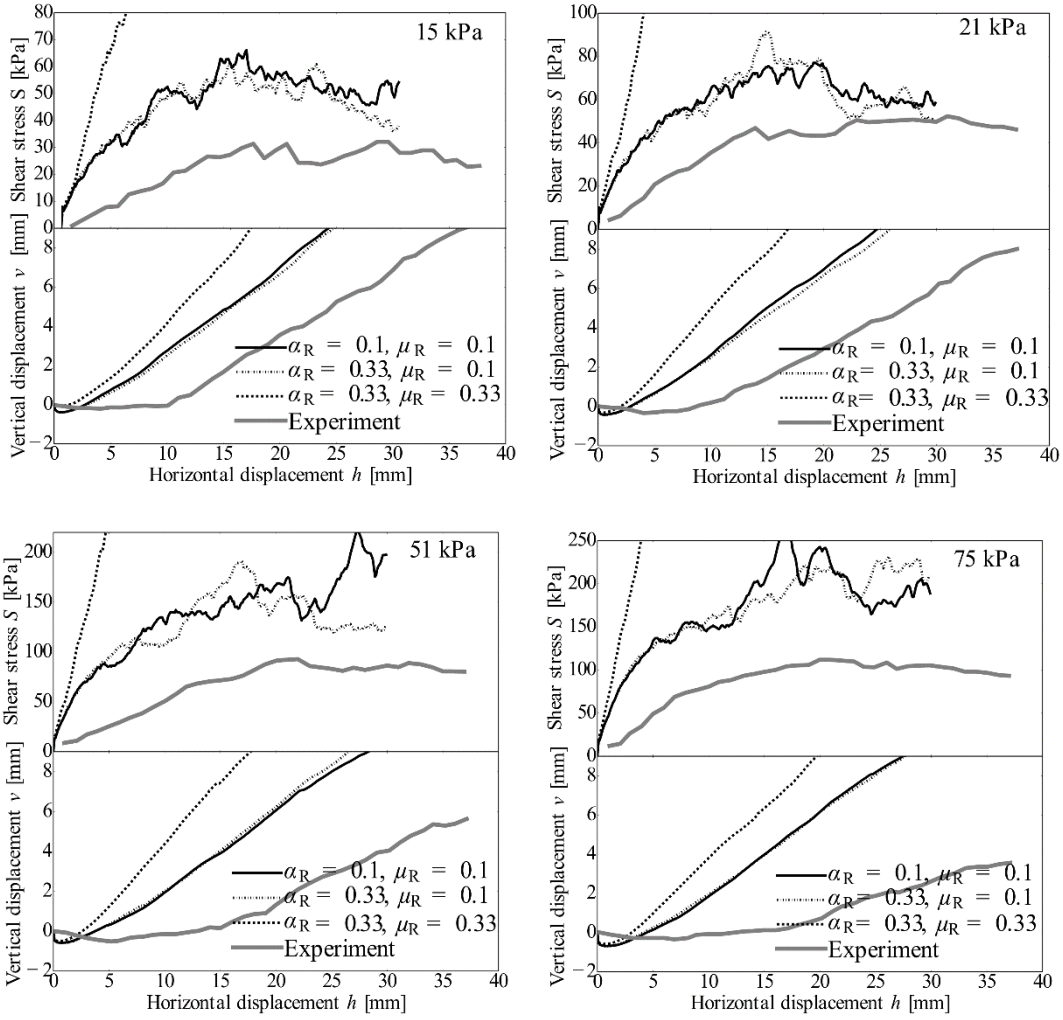

Fig. 9: The average results from 10 realizations of Indaratna's shear; The evolution of shear stress and vertical deformation is shown in separate graphs for four different vertical pressure values

4 CONCLUSIONS

Three different experimental tests were simulated using discrete element method. The main aim of research was to find reasonable rolling parameters usable for simulations of railway ballast. The oedometric test does not show dependence on rolling coefficients, while the next two studied simulations, composite element test and shear test, are strongly dependent on them. However, they show contradictory results. The shear test needs value of μ_R coefficient lower than 0.1, but this value is unusable for Composite element test simulation, since it leads to excessive deformations. The value of μ_R needed for CET is about 0.33. The second rolling coefficient α_R does not play any significant role. This conclusion is supported by all simulated experiments.

The contradiction might be caused by several factors. It might be due to wrong compaction, which is extremely important for granular systems. The experiments were also done on different material, so the rolling coefficients might slightly differ from experiment to experiment. However, it might also indicate incorrect theory behind the rolling resistance phenomena.

ACKNOWLEDGMENT

This outcome has been achieved with the financial support of Brno University of Technology under project No. FAST-J-16-3558. The support is gratefully acknowledged.

LITERATURE

[1] AZÉMA, E., F. RADJAI & G. SAUSSINE. Quasistatic rheology, force transmission and fabric properties of a packing of irregular polyhedral particles. *Mechanics of Materials.* 2009, Vol. 41, pp. 729-741.

[2] BOURRIER, F., F. KNEIB, B. CHAREYRE & T. FOURCAUD. Discrete modeling of granular soils reinforcement by plant roots. *Ecological Engineering.* 2013, Vol. 61, pp. 646-657.

[3] BROWN, S. F., J. KWAN & N. H. THOM. Identifying the key parameters that influence geogrid reinforcement of railway ballast. *Geotextiles and Geomembranes.* 2007, Vol. 25, pp. 326-335.

[4] CLEARY, P. W. DEM prediction of industrial and geophysical particle flows. *Particuology.* 2009, Vol. 8, pp. 106-118.

[5] ELIÁŠ, J. Simulation of railway ballast using crushable polyhedral particles. *Powder Technology.* 2014, Vol. 264, pp. 458-465.

[6] ENGENZINGER, CH., R. SEIFRIED & P. EBERHARD. A discrete element model predicting the strength of ballast stones. *Computers & Structures.* 2012, Vol. 108-109, pp. 3-13.

[7] HOANG, T., P. ALART, D. DUREISSEIX & G. SAUSSINE. A domain decomposition method for granular dynamics using discrete elements and application to railway ballast. *Annals of Solid and Structural Mechanics.* 2011, Vol. 2, pp. 87-97.

[8] HÖHNER, D., S. WIRTZ & V. SCHERER. Experimental and numerical investigation on the influence of particle shape and shape approximation on hopper discharge using the discrete element method. *Powder Technology.* 2013, Vol. 235, pp. 614-627.

[9] INDRARATNA, B., N. NGO, C. RUJIKIATKAMJORN & J. S. VINOD. Behavior of fresh and fouled railway ballast subjected to direct shear testing. *International Journal of Geomechanics.* 2014, Vol. 1, pp. 34-44.

[10] JIANG, M. J., H.-S. YU & D. HARRIS. A novel discrete model for granular material incorporating rolling resistance. Computers and Geotechnics. 2005, Vol. 32, pp. 340-357.

[11] JIANG, M. J., Z. SHEN & J. WANG. A novel three-dimensional contact model for granulates incorporating rolling and twisting resistances. *Computers and Geotechnics.* 2015, Vol. 65, pp. 147-163.

[12] LIM, W. L. & G. R. McDOWELL. Discrete element modelling of railway ballast. *Granular Matter.* 2005, Vol. 7, pp. 19-29.

[13] McDOWELL, G. R. & J. P. DE BONO. On the micro mechanics of one-dimensional normal compression. *Géotechnique.* 2013, Vol. 63, pp. 895-908.

[14] MINDLIN, R. D. Compliance of elastic bodies in contact.. *ASME J Appl Mech.* 1949, Vol. 16, pp. 259-268.

[15] ŠMILAUER, V. et al. *Yade Documentation..* The Yade Project, 2016.

[16] WANG, X. L. & J. C. LI. Simulation of triaxial response of granular materials by modified DEM. *Science China Physics, Mechanics & Astronomy.* 2014, Vol. 57, pp. 2297-2308.

[17] WANG, Z., G. JING, Q. YU & H. YIN. Analysis of ballast direct shear tests by discrete element method under different normal stress. *Measurement.* 2015, Vol. 63, pp. 17-24.

[18] ZHAO, S., X. ZHOU, W. LIU & CH. LAI. Random packing of tetrahedral particles using the polyhedral discrete element method. *Particuology.* 2015, Vol. 23, pp. 109-117.